particles

Communication

Transforming DIY Geiger Counter Kits into Muon Detectors for Education and Scientific Exploration

Marco Arcani [1,*], Domenico Liguori [2], Andrea Frassà [3], Altea Renata Maria Nemolato [4], Omar Del Monte [5] and Cesare Guaita [6]

[1] Astroparticle Detectors Array Laboratory, GAT Astronomical Center, 21049 Tradate, Italy
[2] INFN, National Laboratories of Frascati, Associated Group of Cosenza, IIS Liceo Scientifico "Patrizi", 87062 Cariati, Italy; mim_lig@alice.it
[3] Dipartimento di Fisica, Università di Torino, 10124 Torino, Italy; andrea.frassa@unito.it
[4] Dipartimento di Scienze e Tecnologie Ambientali, Biologiche e Farmaceutiche, Università Degli Studi Della Campania "Luigi Vanvitelli", 81100 Caserta, Italy; altearenatamaria.nemolato@studenti.unicampania.it
[5] VVF, Corpo Nazionale dei Vigili del Fuoco, 15121 Alessandria, Italy; omar.delmonte@vigilfuoco.it
[6] GAT Tradate–Planetarium "Ulrico Hoepli", 20121 Milano, Italy; c.guaita@libero.it
* Correspondence: marco.arcani@astroparticelle.it or info@arcarth.com

Abstract: Any Geiger counter can be used as an effective cosmic ray detector on its own. In fact, it is known that even in the absence of a radioactive source, the instrument detects what is known as background radiation, which consists of various types of ionizing particles present in the environment. Remarkably, it is estimated that up to 15% of this background radiation is attributable to cosmic rays, high-energy particles originating from outer space. The remaining radiation detected by the Geiger counter originates from terrestrial sources, such as natural radioactivity in the ground and in the air. The main goal of this project is to build a muon detector for scientific and educational purposes using two commercial DIY Geiger counter kits and just a few additional components. To identify cosmic radiation from terrestrial radiation and improve the accuracy of cosmic ray measurements, the use of a coincident circuit is essential. This coincident circuit was introduced in cosmic ray physics by Walther Bothe and Bruno Rossi in the early 1930s and allows for the detection of a subatomic particle passing through two or more sensors, thereby reducing false positives and enhancing the reliability of cosmic ray detection. The following idea is an alternative replica of our AMD5 detectors, instruments that we have been using for years to teach and perform scientific experiments in the cosmic ray field under the umbrella of the ADA project (2023 Particles, Arcani et al.). The resulting device, named AMD5ALI, offers a reliable and inexpensive solution for the same goal, making it a valuable tool for both educational purposes and scientific surveys. Practical applications range from cosmic ray physics to radioactivity, including the relationship between cosmic ray flux and meteorology, the zenithal effect, the Regener–Pfotzer curve in the atmosphere, and the anti-correlation of cosmic particle intensity with solar activity.

Keywords: muon detector; cosmic rays; DIY Geiger counter; educational tools; scientific exploration

check for updates

Citation: Arcani, M.; Liguori, D.; Frassà, A.; Nemolato, A.R.M.; Del Monte, O.; Guaita, C. Transforming DIY Geiger Counter Kits into Muon Detectors for Education and Scientific Exploration. *Particles* **2024**, *7*, 603–622. https://doi.org/10.3390/particles7030034

Academic Editor: Francesco Maria Follega

Received: 22 May 2024
Revised: 9 July 2024
Accepted: 11 July 2024
Published: 12 July 2024

1. Introduction

Cosmic rays are high-energy particles that originate mainly from extraterrestrial sources outside our solar system. These particles travel through space at velocities close to the speed of light, reaching Earth from various astrophysical sources such as supernova remnants and active galactic nuclei. They can mainly be divided into three categories: solar (SCR), galactic (GCR), and extragalactic (EGCR). There is also a distinction between cosmic rays originating in space and those generated within Earth's atmosphere by the interactions of cosmic particles with atoms of air. The former are termed "primary cosmic rays", while the latter are referred to as "secondary cosmic rays". Primary cosmic rays are composed of protons (89%), alpha particles (10%), heavy nuclei, and electrons (both negative and positive). Primary cosmic rays interact with magnetic fields due to their charged nature, causing complex motions in space. As a result, the magnetic fields of the Earth, the Sun, and galaxies have various effects on them, including the solar modulation effect and the latitude effect on Earth. When primary cosmic rays enter the atmosphere, they collide with atmospheric atoms, initiating a cascade or shower of secondary cosmic rays. Depending on the energy of the primary particle, these showers can sometimes reach significant extension and particle density at ground level, known as extensive air showers (EAS). A cosmic-ray shower is composed of various types of particles. Among all the secondary particles generated at the top of the atmosphere, pions are the most abundant. Neutral pions decay via gamma rays ($\pi_0 \rightarrow 2\gamma$) with a mean life of 8.4 $\times$ 10^{-8} ns at rest, while charged pions have a mean life at rest of 26 ns and decay into muons and neutrinos through the process:

$$\pi^+ \rightarrow \mu^+ + \nu_\mu \text{ and } \pi^- \rightarrow \mu^- + \overline{\nu}_\mu. \tag{1}$$

For kaons, the scenario is similar, but their multichannel degradation mechanisms are more intricate. Both charged pions and, to a lesser extent, kaons are the main sources of muons. Muons are the most penetrating particles and are considered the "hard" component of secondary cosmic rays. At sea level, muons are the dominant component. The mean life of muons at rest is short, approximately 2.2 $\times$ 10^{-6} s, but they survive down to sea level because of relativity time dilation. Approximately 80% of the charged component of secondary cosmic rays at sea level are muons; their flux amounts to 70 $\text{m}^{-2}\cdot\text{s}^{-1}\cdot\text{sr}^{-1}$. According to their mean life, muons can decay, producing electrons and neutrinos:

$$\mu^+ \rightarrow e^+ + \nu_e + \overline{\nu}_\mu \text{ and } \mu^- \rightarrow e^- + \overline{\nu}_e + \nu_\mu. \tag{2}$$

Electrons, positrons, and photons take part in the electromagnetic component of the central part of a shower, named the electromagnetic (or electrophotonic) cascade. There are multiple sources of this process: decay of secondary particles, such as neutral pions and muons; bremsstrahlung radiation; pair production; inverse Compton scattering; and others. The electromagnetic component is absorbed rather easily and is therefore called the "soft" component. In addition to muons, other secondary cosmic rays that reach the ground include photons and electrons, some hadrons, and a few heavy nuclei (Figure 1).

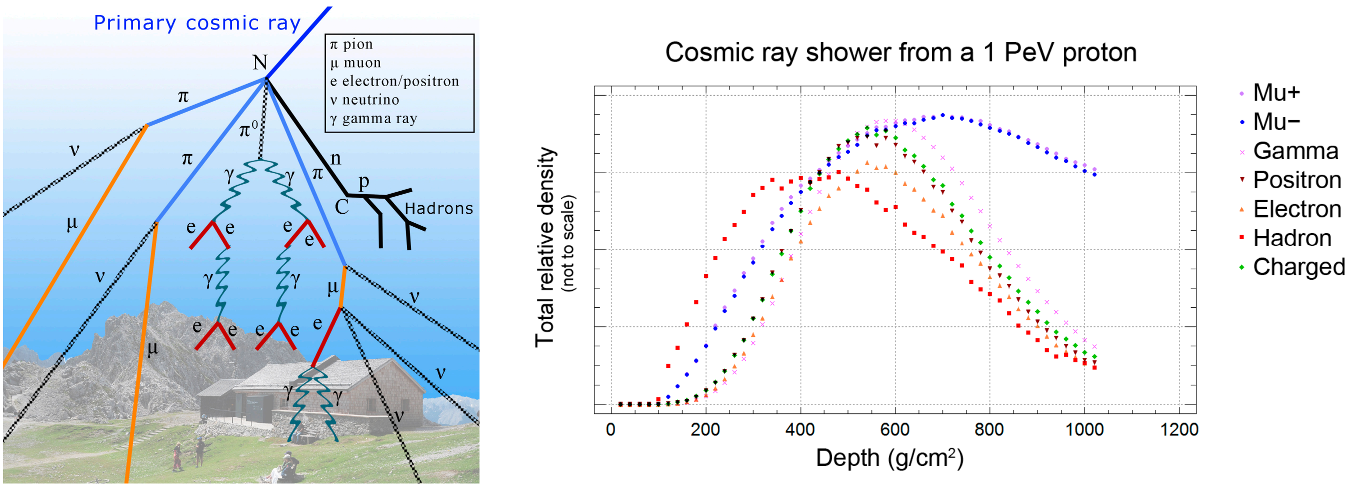

(**a**) (**b**)

Figure 1. Distribution of particles in an atmospheric shower: (**a**) artistic image of an atmospheric shower; (**b**) development of secondary particles in a shower from a single vertical proton carrying 1 PeV of energy (total density versus atmospheric depth). The plot highlights that at ground level, the main component of secondary cosmic particles consists of muons (CORSIKA model simulation by the authors).

Interactions with atoms in the atmospheric air have a strong impact on the development of a shower. The atmosphere's column density is roughly 1030 g·cm^{-2} (about 1010 hPa). For particles with inclined trajectories, the thickness of the atmosphere increases significantly; this is known as the zenith effect. The thickness of the atmosphere can be expressed in units of radiation depth and radiation length. The radiation depth (or interaction depth) is denoted by "X" and is measured in g·cm^{-2}, representing the distance traveled by a particle in a medium times the density "ρ" of that medium. The radiation length "Λ" (in cm) is the distance over which a particle's energy is reduced to $1/e$ of its original energy, or by 36.78%. The number of particles in an air shower decreases exponentially with increasing atmospheric depth and can be described generally as follows:

$$N = N_0 e^{-\frac{X}{\Lambda\rho}}. \tag{3}$$

Primary cosmic rays interact with atmospheric atomic nuclei at altitudes around 15 to 20 km (100 hPa), which can lead to the initiation of electromagnetic and/or hadronic cascades, depending on the energy and type of particle involved. A generic relation, dE/dX, can be used to illustrate the energy loss of cosmic particles in the atmosphere. Every charged particle undergoes various kinds of energy-losing and electromagnetic interactions with the medium through which it traverses. The mass and energy of the projectile, as well as the characteristics of the target, determine the importance of the various processes. Among charged particles, the most common mechanisms for energy loss are ionization and excitation, bremsstrahlung radiation, Cherenkov radiation, inverse Compton scattering, and more. The rate of energy loss by ionization varies logarithmically with energy. To determine such energy loss, the Bethe–Bloch formula is often employed [1]:

$$-\frac{dE}{dx} = 4\pi N_a r_e^2 m_e c^2 z^2 \frac{Z}{A}\frac{1}{\beta^2}\left[\frac{1}{2}\ln\left(\frac{2m_e c^{2\beta^2}\gamma^2 W_{max}}{I^2}\right) - \beta^2 - \frac{\delta(\beta\gamma)}{2}\right]. \tag{4}$$

This equation is commonly applied for a moderately relativistic particle with charge ze that interacts with matter, characterized by atomic number Z and atomic weight A. The relation helps us to understand and quantify the energy loss experienced by charged particles. For instance, the energy loss due to the ionization and atomic excitation of a single muon traversing the atmosphere in a vertical direction is 2.2 GeV. Hence, every single muon at sea level carries at least 2.2 GeV of energy (4 GeV on average). This can be compared with the energy carried by particles from natural radioactivity, which typically have energies on the order of a few MeV, representing a ratio of approximately three orders of magnitude (a factor of 1000). Any sensor employed to detect cosmic rays is sensitive to a wide range of radiation energies. Thus, ground-based cosmic ray detectors can measure not only muons but also other ionizing particles present in the cosmic ray showers. To selectively measure cosmic rays and exclude other particles, it is necessary to stack two or more sensors and consider only the particles that pass through them simultaneously, a method known as coincidence detection. Any cosmic ray detector works on this coincidence technique invented by Walther Bothe and Hans Geiger and then perfected by Bothe and Rossi in order to use three sensors and more [2]. Cosmic ray detectors based on Geiger-Müller tubes (GMTs) use the same historical coincidence method and are sensitive to low radiation, including X-rays with energies as low as a few keV. Alternatively, a thick lead shield (provided it is pure—not radioactive) can be used to block lower-energy particles, or both methods can be employed in combination. Muons, due to their high energies, can penetrate deep material thicknesses, whereas particles produced by natural radioactivity are typically stopped by the first sensor itself or by the lead shielding. It is important to note that detectors of this type can only record the number of events or particles, but they cannot measure the energy released by individual particles.

A GMT, in essence, is made of a metal or glass cylinder filled with a low-pressure inert gas. Inside the tube, there are two electrodes: a central wire anode and an outer metal cathode. A high voltage is applied between these electrodes, creating a strong electric field. When an ionizing particle, such as an electron, enters the tube, it causes the gas atoms to ionize, resulting in the creation of ion pairs (positive ions and free electrons). The high voltage between the electrodes accelerates the free electrons towards the anode. As they move towards the anode, each electron gains enough energy from the electric field to ionize additional gas atoms through collisions. This process is known as the avalanche effect, where a large number of ion pairs are produced along the path of the radiation. This electric current inside the tube causes a drop in the voltage applied to the tube, so it can be converted into an electric pulse and counted as a particle. More than one mechanism is involved in the ionization of the gas. For beta particles, the ionization is induced directly by collisions with gas atoms. For both low X and gamma rays, the mechanism involved is photoionization of the gas atoms. For high energy of the same type, the ionization of the gas is rather caused by electrons ejected by photoemission at the inner surface of the cathode cylinder.

Detection efficiency for a GMT varies with the type of incident particle or radiation and its energy. The efficiency of a counter, defined as the probability that a discharge is initiated by a particle crossing the sensitive volume, has been found to be less than unity for two reasons. First, a particle may pass through a counter without generating any ions. This can occur if the path of the particle through the counter is shorter than the mean free path for an ionizing collision (which is not the case for cosmic rays) or due to fluctuations (e.g., the dead time of the GMT). Additionally, the efficiency depends on the type of gas used and increases with the pressure inside the tube. If "k" represents the average number of ionized electrons by the crossing particle, the efficiency "G" can be defined as follows [3]:

$$G = 1 - e^{-k}, \tag{5}$$

where the exponent can be expressed as $k = s \cdot l \cdot p$, with "l" being the particle path through the tube, "p" being the pressure of the gas, and "s" being the "specific ionization". This last term is derived empirically and can be found in tables. In a standard GMT, the efficiency for beta particles and high-energy electrons can be near 100%, while for high-energy photons (30 keV $\div$ 1.25 MeV), it can be as low as a few percent. Cosmic muons are known to be less ionizing than electrons according to the Bethe–Bloch equation, and this is mainly due to their high momentum. However, historical experiments have shown the construction of dedicated GMTs with 98% efficiency for detecting muons.

In the last decade, there has been a great expansion of educational cosmic ray detector projects, mainly based on silicon photomultipliers (SiPMs) coupled to small scintillators. Among them are CosmicWatch [4], CosmicPi [5], LoCoMoTe [6], and ArduSiPM [7]. The motivation for building a cosmic ray detector using a DIY Geiger counters comes from several key factors that make this approach particularly appealing and practical. One of the primary motivations is cost containment. Modern cosmic ray detectors, which rely on scintillators and photomultipliers (PMTs or SiPMs), can be quite expensive, often necessitating specialized components and sophisticated electronics. However, by opting for GMTs instead, it becomes possible to significantly reduce the overall cost (below 100 euros) of constructing a cosmic ray detector while still obtaining a portable and functional instrument. Although the use of GMTs may seem outdated today, they are still utilized even in cosmic ray physics [8,9]. DIY Geiger counter kits, in the last few years, have become widely available from various suppliers and can be easily purchased online or from local electronics stores. This widespread availability ensures that researchers, educators, and enthusiasts have easy access to the necessary components, making it easier to embark on projects involving muon detection without facing supply chain limitations or procurement challenges. Geiger counters are simple and generally affordable, this is another compelling motivation for their use in building cosmic ray detectors. These counters are designed to be user-friendly and relatively straightforward to assemble and operate, even for individuals with limited technical expertise or experience in electronics. The simplicity of DIY Geiger counters makes them accessible to a broader audience, including students and educators, who may not have extensive background knowledge in particle physics or detector technology but are interested in learning about and exploring cosmic rays or incorporating cosmic ray detection into educational curricula.

We have previously developed a cosmic ray detector named AMD5 (AMD stands for Astroparticle Muon Detector, plus version number), which has been in use since 2012. This detector was initially constructed during the centenary of the discovery of cosmic rays, and a predecessor version called AMD4 was utilized during the VHANESSA expedition, which involved flying on a hot air balloon to repeat the Victor Hess experiment [10]. Over the years, the AMD5 detector has undergone improvements, and with its latest version, we have achieved significant and interesting results: evidence of the Forbush effect, absorption of muons in matter (water, concrete, and metals), seasonal effects, and more (see Supplementary Materials). This detector has proven to be a valuable tool for teaching modern physics, especially in secondary educational settings such as high schools and colleges. To date, more than twenty AMD5 and similar detectors have been installed in Italy, Switzerland, Luxembourg, and even Iceland as part of a larger project called "Astroparticle Detector Array" (ADA), a network that aims to detect high-energy cosmic rays [11]. The AMD5 detector is constructed using two GMTs of Soviet production type SBM 20. Unfortunately, due to the ongoing conflict between Russia and Ukraine, these sensors are almost impossible to find. This was also a motivation for looking at the Chinese market in search of a substitute for such GMTs.

In an AMD5 detector, the two GMTs are stacked one over the other, and the signal from the sensors is captured and sent to an electronic board, where a logic gate "and" functions as a coincident circuit. The processed signal is then sent to different outputs, allowing for connectivity to a computer via USB; a microcontroller via TTL logic; or a sound card.

The availability of these outputs enables the use of various software options for Geiger counters that are already available on the market, including some applications for smartphones. Additionally, we have developed our own software called AstroRad for counting the flux of cosmic particles. AstroRad serves as a data logging tool, generates graphs from readings, and offers additional functionalities to facilitate data analysis and statistics.

While we are developing a new electronics board and other improvements for the AMD5, building upon the success and capabilities of our detector, we present an alternative and simple way to obtain a replica of a similar instrument. This alternative approach provides the opportunity to construct a detector that we named AMD5ALI, leveraging the proven design and functionalities of our existing detectors. Additionally, we provide a comparison between the two devices to highlight their respective features. Our main intention is to promote further scientific exploration and educational initiatives in the field of astroparticle physics.

2. Materials and Methods

2.1. Muon Detector AMD5 Features

Bruno Rossi referred to this type of detector as a "cosmic ray telescope" [12]. Indeed, stacking two or more tubes creates a specific field of view, or geometry, for the instrument. In the case of the AMD5 detector, the distance between the tubes was arbitrarily chosen to be 6 cm. As a result, the instrument has a radial angle field of approximately 18°, given that the diameter of the GMTs is about 1 cm, and an axial angle field of view of about 105°, considering that the length of the useful (sensitive) GMT part is 7.8 cm. Using the following equation, is possible to calculate the solid angle view of the detector [13]:

$$\omega = 4\sin^{-1}\left(\frac{lb}{\sqrt{\left(l^2+4d^2\right)\left(b^2+4d^2\right)}}\right), \tag{6}$$

where "*l*" is the length of the tubes, "*b*" is the width (diameter), and "*d*" is the semi-distance. In this way, we have found that the telescope "sees" a solid angle of approximately 0.52 steradians (sr) (Figure 2).

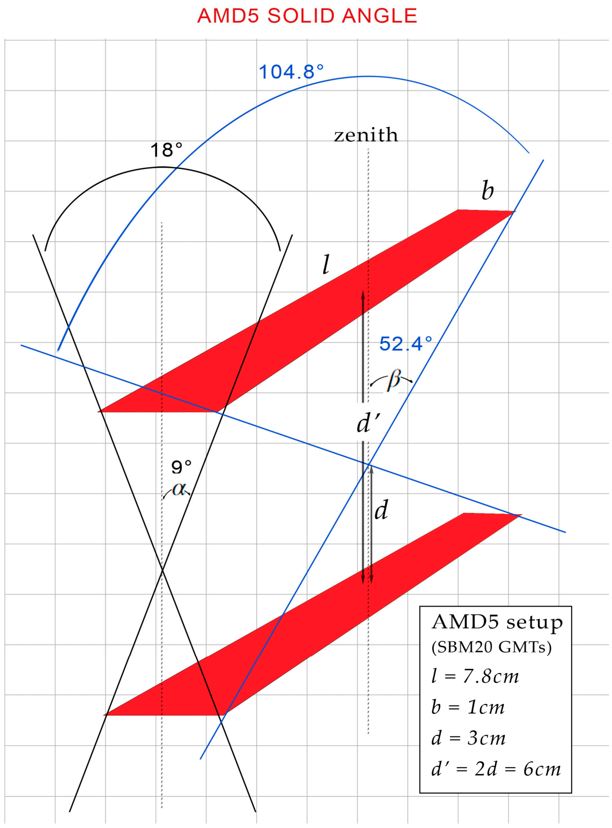

Figure 2. Schematic representation of the field of view by the AMD5 detector.

As we make several detectors with different configurations, we have an online tool to calculate the solid angle for any type of detector: see "https://www.astroparticelle.it/login/page10_eng.asp (accessed on 16 May 2024)". This tool is also implemented in our own ADA app for Android smartphones. As previously seen, particle detectors are designed according to the coincidence method to record the passage of a particle in two or more interaction channels. This method helps to distinguish genuine cosmic ray events from natural background radiation. Since the pulse from a GMT is usually quite short and noisy, it is common practice to extend the duration of the pulse. Such a time is called the "coincidence window". If the two pulses arrive overlapping, the event is considered a cosmic particle or a muon. One of the initial considerations was determining the timing for the coincidence window between the signals from the two GMTs, as an excessively long time window would result in recording numerous environmental particles.

The first prototype made use of a coincidence time window of 100 ms. Using a time between 20 and 100 ms, the results provided substantially similar outcomes. A test involving the placement of weak radioactive elements in close proximity to the detector (a few tens of centimeters away) did not result in a significant increase in coincidences.

Subsequently, the coincidence timing for the AMD5 detector was adjusted to the current value of approximately 60 ms. Over time, we observed that some sites where AMD5 detectors were installed had elevated levels of radon. This element is problematic because it wraps the GMTs, and its decay products generate particles that can cause false coincidences. This sneaky effect introduces a modulation in the cosmic ray flux. To address this issue, an alternative time window of approximately 190 µs (0.2 ms) was introduced. This value corresponds about to the dead time of the GMT (SBM20); therefore, it is the minimum possible value. Thanks to this modification, the issue related to radon has been significantly mitigated, although not entirely solved.

To calculate the rate of accidental coincidences, we can employ methods that have been traditionally used when Geiger–Müller tubes (GMTs) are extensively utilized for the study of cosmic rays. Janossy describes two equivalent methods, which, in our case, can be expressed as follows [14]:

$$A = 2N^2 \cdot \tau, \tag{7}$$

where A is the number of false coincidences per second, N is the GMT rate (cps), and τ is the acquisition time. Using the GMT model SBM20, we have $N = 0.4 \pm 0.01$ cps. Therefore, with $\tau = 60$ ms, we obtain $A = 0.02$. In contrast, for $\tau = 0.2$ ms, we calculate $A = 6.4 \times 10^{-5}$. This indicates that with the first time window (we call it CW1), the rate of false coincidences (regarding N) is approximately 5%, whereas with the second time window (CW2), the rate significantly decreases to 0.016%. Table 1 shows the data for both detectors.

Table 1. False coincidence rate (for AMD5 CW2 = 0.2 ms, while for AMD5ALI CW2 = 1 ms).

Detector	N (Average) [cps]	A-CW1 (60 ms) [cps]	A-CW2 (0.2 ms/1 ms) [cps]
AMD5 (SBM20 GMTs)	$4.01 \times 10^{-1} \pm 0.01$	1.93×10^{-2}	6.43×10^{-5}
AMD5ALI (J305 GMTs) [a]	$3.72 \times 10^{-1} \pm 0.01$	1.66×10^{-2}	2.77×10^{-4}

[a] See Section 2.3.

These calculations must always be considered with caution. "False coincidences" can also be produced by different but contemporary cosmic particles. For example, two muons can affect, at the same time, the two sensors with different inclinations, and other secondary (tertiary) particles can be produced in the detector via scattering or recoil interaction with the metal parts of the detector itself.

The motivation for maintaining two coincidence windows relies on the dimensions of the detection surface, which are relatively modest compared to professional muon detectors. The larger window was chosen for standard operation as a compromise, ensuring an adequate event rate for reliable scientific results despite the small amount of natural ionizing radiation detected within cosmic rays. This dual-window approach allows the detector AMD5 to be flexible for different experiments, optimizing the balance between sensitivity to cosmic ray muons and rejection of environmental noise. The use of a large coincidence window, despite its drawbacks, is justified to achieve a satisfactory event rate and ensure the reliability of scientific data in the context of the detector's limitations and operational requirements. However, for optimal performance in focused experiments, we recognize the need to use the shorter available coincidence window. The average flux of cosmic particles measured by the AMD5 detector is approximately 5.3 cpm·sr with the standard time window (CW1) of 60 ms and about 1.2 cpm·sr with the minimum time window (CW2) of 0.2 ms.

2.2. The Zenith Angle Dependence Test

The intensity of cosmic rays is strongly dependent on the alt-azimuth system of coordinates. If the orientation with respect to the azimuth can be neglected (apart from the east-west effect, which also depends on the latitude), the orientation with respect to the zenith angle is dominant instead. The more their trajectory is inclined, the more matter particles have to pass through, and by losing their energy, they become extinct more quickly (Figure 3).

Cosmic rays, therefore, decrease in number with an increase in the zenith angle. For certain angles of incidence and at high altitudes, even the curvature of the Earth must be taken into account. The intensity of the measured flux depends on the following relation [15]:

$$I_i(\theta) = I_i(0^\circ) cos^{ni}(\theta), \tag{8}$$

where the exponent "*ni*" is a function of the energy, the kind of particle, and the thickness of the air, which is indicated as interaction depth (X), which is measured in g·cm^{-2}. Generally, this proportionality can be approximated to

$$I(\theta) = I(0^\circ)cos^n(\theta). \tag{9}$$

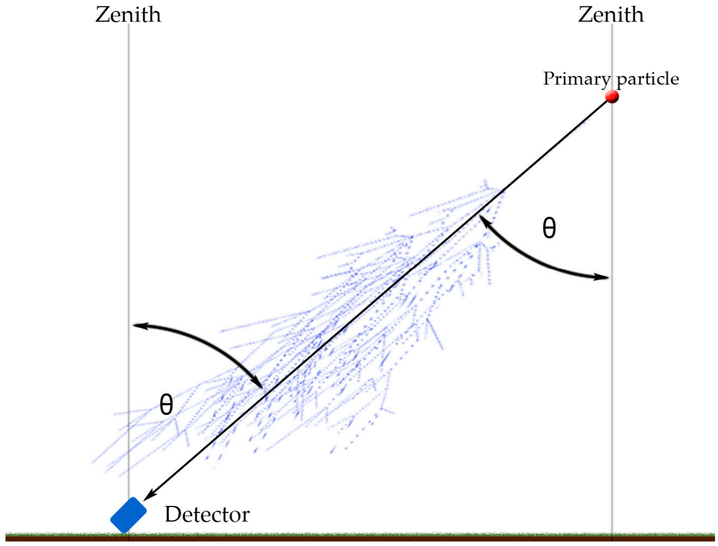

Figure 3. Inclination of the detector with respect to the zenithal angle.

For neutrons, "n" is approximately equal to 3.5 (1971, Heidbreder et al. [16]). For electrons, experimental measurements indicate a value of "n" equal to 2, where it becomes 3.6 for particles with energies equal to or greater than 100 MeV. For muons, which are the particles of our main interest, the issue is trickier. Muons arise from the decay of pions and kaons; thus, their production depends on the interaction with the air of their progenitors, which have different behaviors; furthermore, the energy spectrum of muons at sea level is very broad. In any case, the expression (4) is still valid; however, for muons, "n" is directly proportional to the momentum (ρ). For example, if the average of ρ is in the range of 1 GeV/c, "n" is equal to 1.85. At sea level, for muons around 3 GeV of energy (say, their minimum value at sea level), the distribution can more simply be considered proportional to the cos^2 of the zenith angle θ (Figure 4).

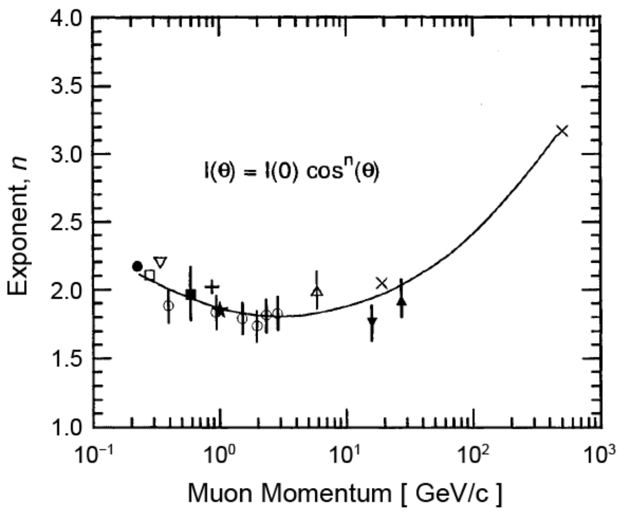

Figure 4. Graph obtained from experimental data, it shows the value of n as a function of the moment in GeV (Bhattacharyya, 1974 [17]).

A simple and valid test to check the good functioning of any muon detector is to collect the rate of muon at a zenith angle equal to 45° and in a vertical position (θ equal to zero). As $\cos^2$ (45°) is equal to 0.5, the ratio between the two measurements must be equal to 0.5. In Table 2, we show the response for the AMD5 detector with both its coincidence windows for 250 counts (minutes).

Table 2. Zenith angle dependence test for AMD5 (uncertainty expressed as standard error).

Coincidence Window	Rate (θ_{0°) [cpm]	Rate (θ_{45°) [cpm]	Ratio
CW1	2.75 ± 0.1	2.01 ± 0.1	0.73
CW2	$5.80 \times 10^{-1} \pm 0.05$	$3.32 \times 10^{-1} \pm 0.03$	0.57

This test confirms that using CW2, the recorded value is pretty much close to the expected result, while using the standard window CW1, the ratio exceeds 0.5 by 46%. As discussed earlier, this discrepancy arises because CW2 allows natural radioactivity to influence the counts, although this effect can be mitigated by extending the counting duration. This example illustrates that, in some types of experiments, a shorter coincidence window is indeed a better choice.

2.3. DIY Geiger Counter Kits

The two commercial DIY Geiger counter kits used for this instrument come from one of the biggest Chinese online stores (aliexpress.com, thus the name AMD5ALI). They do not have a particular code of identification but can be easily found by searching for "Geiger counter kit" and are sold as an assembled or unassembled version. The assembled kit is ready to use after simple operations, one of which is the insertion of the GMT in its dedicated slot. The GMT is labeled as J305 (also M4011). We were not able to obtain information from the manufacturer directly, so the only data available are those published by the sellers (see Table 3).

Table 3. J305 Geiger tube specification.

Type	Glass, Tin Oxide Cathode, Coaxial Cylindrical Thin Shell Structure (Wall Density 50 ± 10 cg/cm^2) 10^{-5}
Application temperature	−40~55 °C
Application detection	Both beta and gamma radiation
γ sensitivity	20 mR/h~120 mR/h
Sensitivity to β Radiation	range 100~1800 changing index/minutes·cm^2 soft β ray [1]
Sensitivity to γ Radiation	0.1 MeV
Background	0.2 pulses/second [2]
Working Voltage	380–450 V
Working Current	0.015–0.02 mA
Length	90 ± 3 mm and 107 ± 3 mm
Diameter	10 ± 0.5 mm

[1] Could be read as cpm/cm^2. [2] Dependent on local natural radioactivity, our measurements did show 0.4 cps on average (see *N* in Table 1).

For unknown reasons, there are two versions under the same code that differ only in their length, one 90 mm long and the other 107 mm long, while the diameter is 10 mm for both. The former is included in these kits, while the latter has exactly the same dimension as the model SBM20 made in Russia, and since it is impossible to buy items from Russia or Ukraine, that model (long version) will likely be the choice for our next AMD5 detectors. Alas, the official electronic diagram is not available; however, it is possible to find some hints on the web [18]. The electronics of the counter provide the power source for the GMT (around 400 V) and include a waveform generator for the output signal (Figure 5).

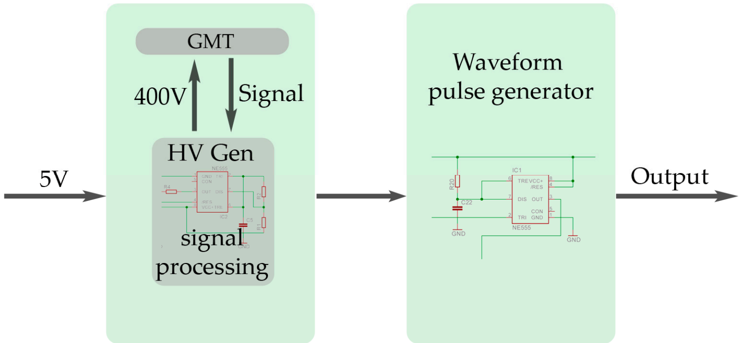

Figure 5. Block diagram for the electronics of the DIY Geiger counter kit.

We have tested the signal output features of the GMT sensors with an oscilloscope, and the results are shown in Figure 6. Each tube's signal is very clean, and the pulse form is nearly triangular, with a very short width of around 20 µs. The output signal from the electronics is a square-wave pulse with a width of about 1 ms (exactly 954 µs). In the assembled version, there is no need for calibration, while the unassembled kit needs the calibration of the high-voltage source and a control on the proper working of the GMT pulse signal [19].

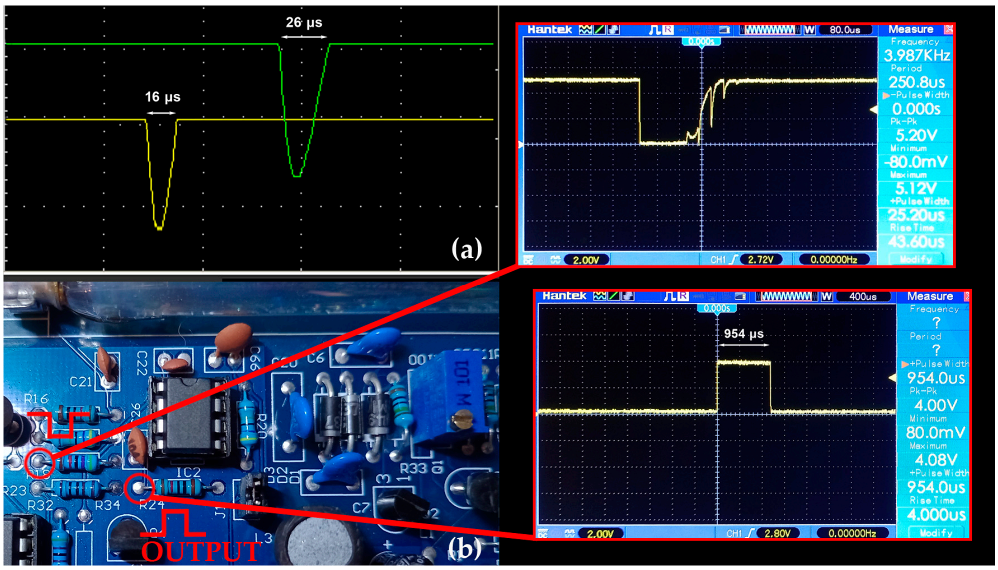

Figure 6. Output signals from the GMTs and the electronic board: (**a**) measurement of the pulse width directly from the GMTs; (**b**) signals from the board as shown, the square pulse of 1 ms width is the final output.

2.4. Hardware Transformation into a Muon Detector

The modifications required to transform the device into a muon detector are relatively straightforward and can be completed quickly in practical terms. After assembling and confirming the proper functioning of both individual counters, it is advisable to proceed with the following tasks by removing the GMTs to prevent any damage. First, four MA3-type screws, each 6.5 cm long, are needed, along with a thin rubber tube, sheath, or tape for insulation. These screws are used to assemble the two boards together and should be wrapped with a sheath or tape to ensure electrical insulation. Care should be taken to ensure there is no connection between the screws and the GMT clips (Figure 7).

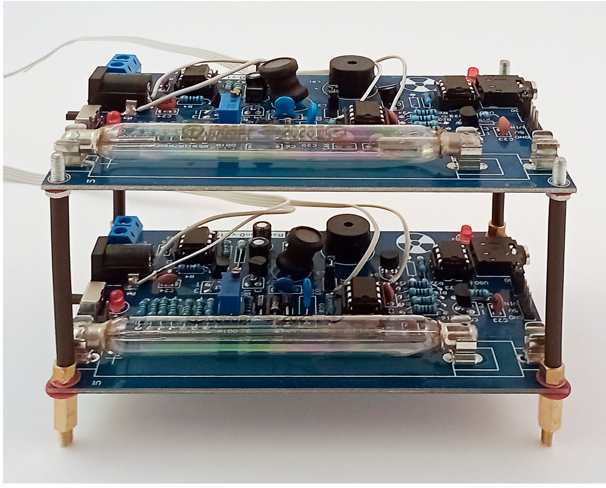

Figure 7. The two boards assembled together.

In order to obtain a solid angle of 0.5 sr as for the AMD5 setting, the distance between the two GMTs should also be 6 cm and can be adjusted by moving the bolts. However, one can choose a different solid angle (e.g., 1 sr), according to equation (1), and therefore a different distance between the two boards (GMTs). The second part requires the construction of the coincidence circuit that is the core of a muon detector.

2.5. The Coincidence Board

This circuit consists of an "and" logic gate, as previously described. The electronics use an IC 4093, which is a quadruple Schmitt trigger NAND gate. The Schmitt trigger configuration usually assures a very clean square wave, even though in this case it is not required as the pulse is already squared. From the two boards, it is indispensable to solder four wires: Vcc (5V), ground, pulse output, and capacitor reference (optional in order to obtain the second time window), as shown in Figure 8a. The whole schematic, with a possible board realization, is shown in Figure 8b.

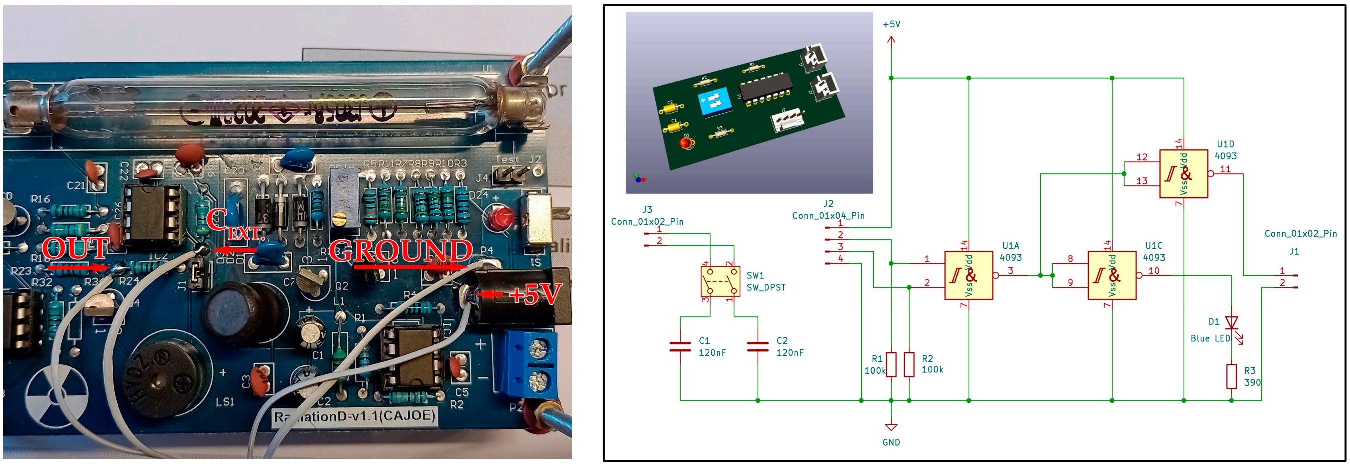

(**a**) (**b**)

Figure 8. Last operations for the construction of the muon detector: (**a**) soldering of four wires towards the coincidence board; (**b**) schematic of the coincidence board and 3D rendering from the KiCad software (release 8.01).

IC 4093-A works as a NAND gate, while IC 4093-C and IC 4093-D (IC 4093-B is not used) work as independent NOT/buffers; the first drives an LED, and the second is actually the output of the muon detector. In normal operation, when the electronics of these Geiger counters detect a particle, they provide an output consisting of a square pulse with a width of 1 ms. So, the detection of a cosmic particle consists of two pulses arriving simultaneously from both counters within 1 ms. As previously mentioned, the AMD5 offers two selectable coincidence windows. We can replicate almost the same features in the AMD5ALI by adding two 120 nF capacitors. This allows us to achieve two coincidence windows, one of 1 ms and the other of 60 ms. It is also possible to shorten the first window to 0.2 ms (as in the original AMD5), but this would require replacing a capacitor on the GMT counter board, which we believe is not necessary as the results in terms of muon detection would be quite similar, according to the previous tests.

Sw1 is the selector used to switch from the short coincidence window to the long one. As can be seen, the switch adds the two capacitors (C1 and C2) in parallel to the original capacitor mounted on each GMT board. Since all the boards are powered by a 5 V power source (any capable of a few hundred mA), the output is compatible with any sort of development board or microcontroller, Arduino included.

We conducted several tests to verify the correct working status. First, we had a problem with a board. Being a cheap product, the PCB is of poor quality, resulting in bad solder joints and missing copper pads and traces. After resolving these issues, the detector started to work properly. The average flux of cosmic particles measured by the AMD5ALI detector is approximately 2.3 cpm·sr with the standard time window (CW1) of 60 ms and about 0.5 cpm·sr with the minimum time window (CW2) of 1 ms. Our first AMD5ALI prototype is shown in Figure 9.

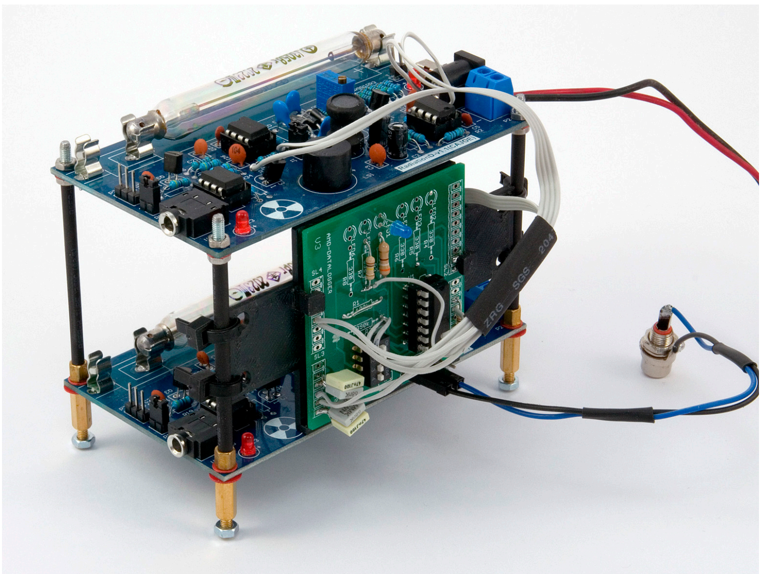

Figure 9. Final version of an AMD5ALI prototype.

3. Results

We made a set of two zenith angle dependence tests (as shown in Section 2.2). In the second test, we decided to add a lead plate, 4 mm thick, between the two sensors in order to obtain any other possible insights. The results are shown in Table 4. For comparison, we added the data related to an AMD5 detector.

The AMD5ALI detector shows a rate that is about half that of an AMD5, despite the fact that the dimensions of the GMTs are similar (they differ only by about 1 cm^2 of useful surface). This discrepancy suggests that the SBM20 sensors may be more sensitive. Regarding the lead shield, there seems to be a degree of energy absorption in each measurement. This means that the lead can cut off some scattered low-energy particles. However, it has only resulted in a noticeable improvement in the ratio data associated with the AMD5ALI (from 0.6 to 0.5); no such improvement is evident in the other detector. To confidently determine the effectiveness of the lead shield, it would require further statistical analysis.

In conclusion, the ratio value evidences that the AMD5ALI definitely works as a muon detector. Of course, these are tiny devices, and their overall rate is low. Nonetheless, one of the strengths of these instruments is their portability in the classroom for educational purposes and their ability to participate in interesting activities such as the International Cosmic Day organized by DESY every year [20]. From a scientific point of view, these kinds of instruments are very useful for long-term measurement and the possibility of comparing the data among them, as in the ADA project. This can potentially lead to interesting results. For instance, in Figure 10, we show the measurements of three detectors placed side by side in the same location for the last entire year: an AMD5, an AMD15 (it differs only for bigger GMTs while having the same geometry), and an AMDRAD (a dosimeter with a single and even bigger GMT).

Table 4. Zenith angle dependence test using the narrow coincidence window CW2.

Detector	Rate (θ_{0°) [cpm]	Rate (θ_{45°) [cpm]	Ratio
AMD5ALI	$2.55 \times 10^{-1} \pm 0.05$	$1.55 \times 10^{-1} \pm 0.05$	0.60
	$2.43 \times 10^{-1} \pm 0.05$ *	$1.23 \times 10^{-1} \pm 0.05$ *	0.50
AMD5	$5.80 \times 10^{-1} \pm 0.05$	$3.32 \times 10^{-1} \pm 0.03$	0.57
	$4.68 \times 10^{-1} \pm 0.04$ *	$2.76 \times 10^{-1} \pm 0.05$ *	0.59

* With the lead shield between the GMTs.

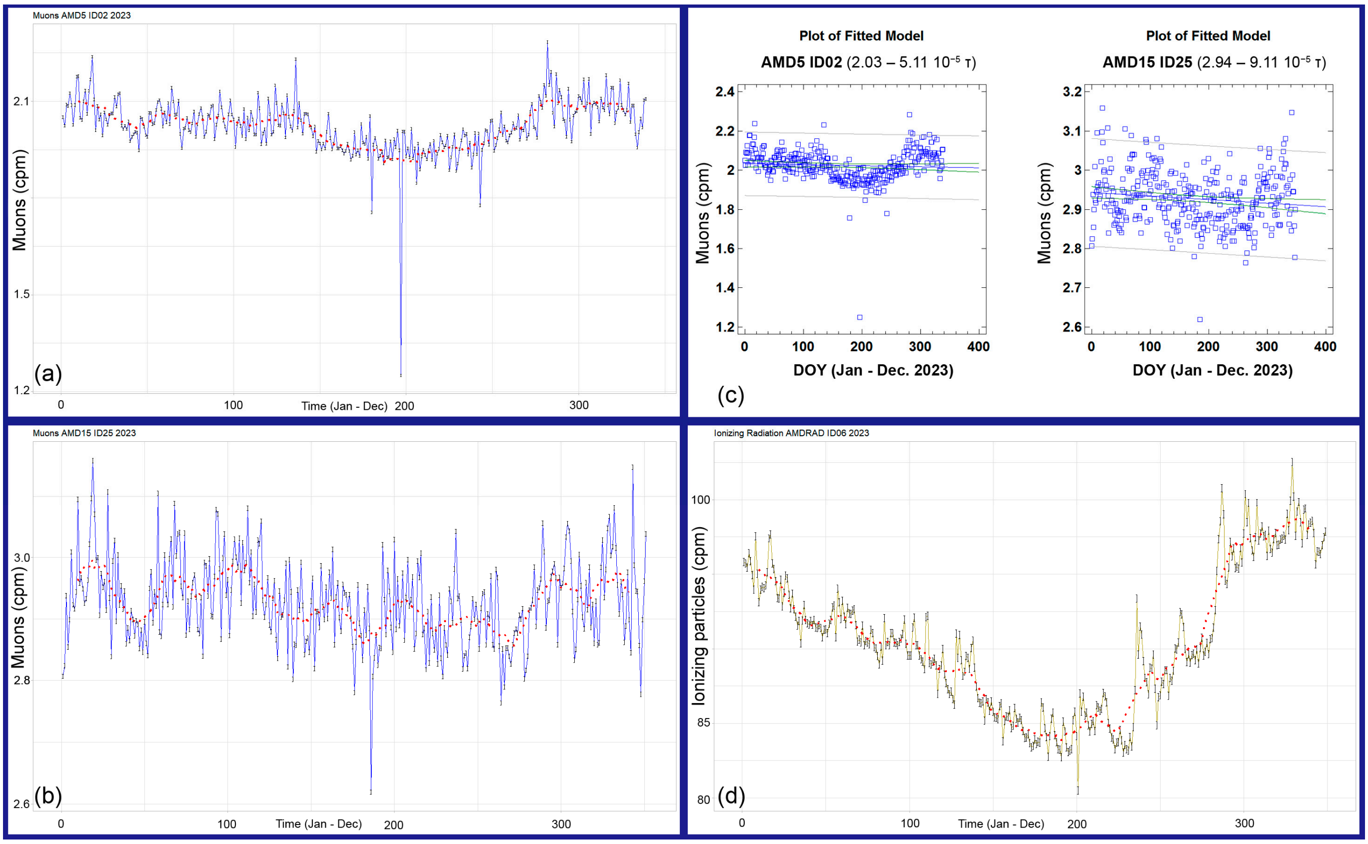

Figure 10. Quick analysis of three detector data sets from January to December 2023 (daily average): (**a**) Muon detector AMD5 Id02 plot; (**b**) Muon detector AMD15 Id25 plot; (**c**) simple regression of the two muon detectors; (**d**) Dosimeter AMDRAD Id06 plot. For (**a**,**b**,**d**), the red dotted line represents a running mean (ADA project network).

A brief analysis shows in both muon detectors the seasonal effect related mainly to the atmospheric temperature (and pressure) that is inversely proportional to the muon flux; indeed, the rate in the summer month is low compared to the winter one [21]. An interesting result is that practically the same seasonal trend is also present in the dosimeter data (AMDRAD), here also expressed in raw counts per minute (cpm). The average count in the period 121–234 (around 1 May–10 August)—certainly the hottest months in our location—is around 85.5 $\pm$ 0.17 cpm, compared to 92.9 $\pm$ 0.23 cpm in the remaining period. The comparison indicates a difference of 8.6% between the two averages. This contribution is in the order of magnitude of the cosmic component (muons), which, as is known, is between 10 and 15% of the total ionizing radiation, so our assumption is that the seasonal effect in this detector coincides with the atmospheric absorption of muons, which also occurs for the other detectors.

The two muon detectors also show that the general trend (linear regression) is slightly decreasing for the last year; this means that the Sun until December 2023 was still rising in its magnetic strength, and maybe even today it has not reached the maximum of its current cycle (see Appendix A). Other features visible in the detector data are currently under assessment. The detectors can be operated to study the relationship between cosmic particles and weather or space weather phenomena. We know that some researchers are using similar simple devices to study the role of cosmic rays in relation to sudden ionosphere disturbances. However, our greatest ambition would be to record signals from the next galactic supernova, and these detectors could potentially do even that.

3.1. Scientific Exploration: Detectors in the Stratosphere

With GMT-based detectors like those in the AMD family of the ADA project, it is possible to carry out several educational experiments. These include measuring the variation in cosmic ray flux as a function of altitude; studying the dependence of muon flux on atmospheric parameters such as temperature, pressure, and humidity; investigating diurnal and seasonal variations in flux rates; assessing the attenuation of cosmic ray intensity through different materials such as water, concrete, or lead [22]; examining the dependence of cosmic muon rates on measurement angles relative to the vertical direction (zenith effect); conducting coincidence measurements to study the geometric acceptance of the detector; and performing measurements of equivalent absorbed dose (see Supplementary Materials). Over the years, these experiences have been carried out in many secondary schools, with remarkable results in terms of teaching. Laboratory activities with cosmic rays arouse great interest among young students and offer them the opportunity to put into practice the theoretical concepts studied in data analysis techniques, programming, and electronics. One of the most important examples in this area was the MoCRiS (Measurement of Cosmic Rays in Stratosphere) project [23]. This experiment involved the students of the fourth and fifth classes of the Scientific High School of Cariati (CS) during the 2022–2023 school year. In an educational approach, a weather balloon was loaded with instruments to study the variation of cosmic radiation flux as a function of altitude. The aim of the experiment was to replicate, using modern methods, the historic measurements conducted by Victor Hess [24] and by Erich Regener and Georg Pfotzer [25,26]. The objective was to introduce pupils to the physical characteristics of near-Earth space, focusing particularly on the ionizing radiation present in the stratosphere as well as its temperature, pressure, relative humidity, UV radiation, and ozone concentration. The measuring instruments were carried aloft by a sounding balloon, which reached an altitude of about 33,200 m. Students were involved in every stage, from designing and constructing the probe to studying the theoretical principles of physics and aerospace technologies. They also participated in the launch of the balloon. The data depicting the variation in cosmic ray flux, measured using an AMD5 detector as a function of atmospheric pressure and consequently altitude, are illustrated in Figure 11.

In this study, we also estimated the equivalent dose value absorbed during the stratospheric flight of the MoCRiS balloon (approximately 33,000 m). This measurement served as a useful introduction to the topic of radiation protection on space flights for the classroom. The calculation of the dose equivalent was conducted using the following relationship:

$$H = C_f \cdot cpm, \tag{10}$$

where H represents the equivalent absorbed dose (mSv/h), and C_f is a calculated conversion coefficient. In our case, we assumed C_f to be equal to 5.8×10^{-3} mSv/h [27]. For the one-hour flight duration, we estimated an equivalent dose of 3.0 ± 0.1 mSv. This can be compared to the approximate 2.4 mSv of natural radiation background (worldwide average annual value) [28] or to the 160 mSv dose absorbed by astronauts during approximately 6 months of orbit around the Earth [29].

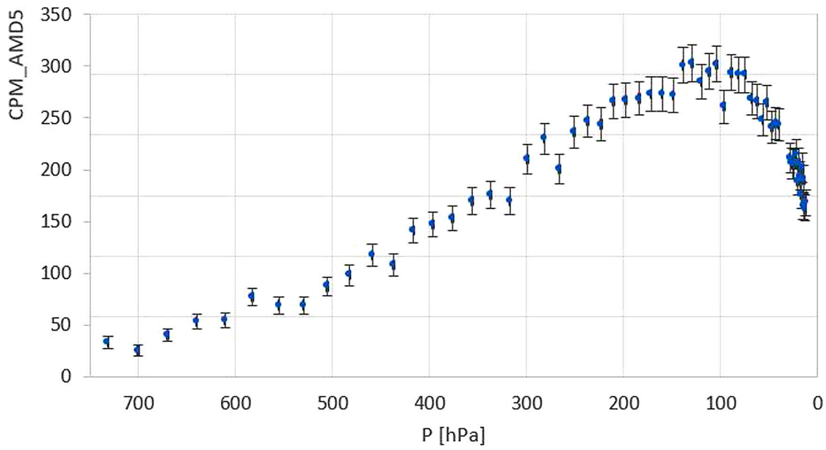

Figure 11. AMD5 counts per minute (cpm for a single GMT) as a function of atmospheric pressure. The counts increase with decreasing atmospheric pressure, indicating the balloon's ascent in altitude. Till about 500 hPa (Hess reached 5200 m), the trend reproduces Hess's results. The counts reach a maximum, replicating the historical findings of Regener and Pfotzer.

3.2. Case Study: A Muon Telescope in the Classroom

Implementing AMD5 detectors for educational purposes offers a versatile tool for various educational settings. One innovative application involves the construction of a muon telescope, a structure capable of rotating and scanning the sky at different angles. In Biella, such a structure was erected last year by mounting the AMD5 detector on a telescope mount, enabling it to span over 90° in zenithal angle. This setup provided a unique opportunity to measure the flux of muons from cosmic rays and explore its dependence on distance from the zenith (Figure 12).

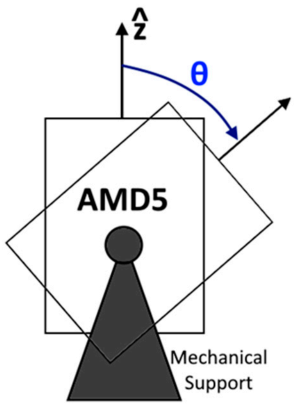

Figure 12. Raw schematic of the mounting for the muon telescope.

Students from diverse academic backgrounds engaged in a range of projects utilizing the muon telescope. They conducted experiments to measure the rate of incoming muons at different angles and applied mathematical models to fit the data. While the results mostly behaved as anticipated, an unexpected phase shift was observed. Subsequent investigations by educators revealed that the room's walls contained traces of radioactive elements, contributing to higher background noise at lower angles. Subtracting the background and fitting the new data yielded no phase shift. Errors are largely overestimated due to the low statistics taken by students; further studies will certainly be performed on larger datasets (Figure 13).

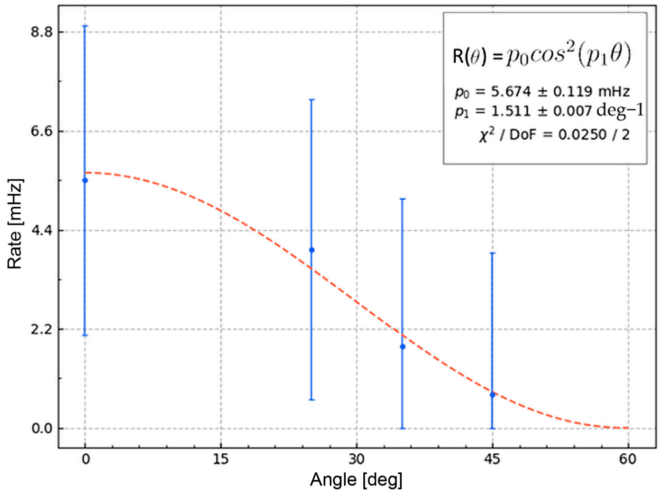

Figure 13. Rate of incoming muon at different angles starting from the zenith. Error bars are calculated following Poissonian statistics, which is the square root of counts, divided by the sampling time.

Impressively, some students ventured further by conducting Monte Carlo simulations to assess the geometric acceptance of the AMD5 detector (Figure 14). Their simulation, assuming a muon direction distribution following a specific pattern and uniform azimuthal angle distribution, yielded valuable insights. By propagating generated particles and counting only those that interacted with the second layer of detectors, they determined the detector's geometric acceptance: 0.03 ± 0.06.

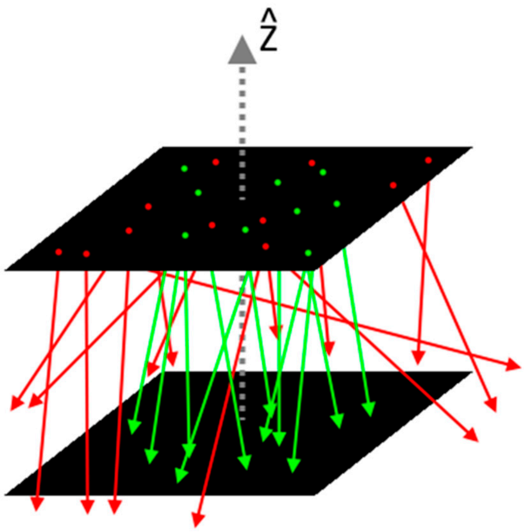

Figure 14. The figure shows how the Monte Carlo was conducted: particles were generated on the top detector and then moved in a random direction. Geometric acceptance is calculated as a fraction of those crossing the second layer (green ones) over the total number of particles (red and green).

Upon completion of these projects, feedback from both students and educators was overwhelmingly positive. Students expressed fascination with the hands-on, problem-solving approach that is inherent in experimental physics, finding it more engaging than traditional textbook learning. Educators appreciated the opportunity to introduce complex concepts in particle physics through a tangible, visual tool, bridging the gap between theory and practice in the classroom.

4. Discussion

In today's rapidly evolving scientific landscape, there are numerous avenues for promoting scientific exploration. Among these, the transformation of DIY Geiger counter kits into muon detectors stands out as one of the most accessible and straightforward methods. These detectors provide a convenient starting point for enthusiasts, educators, and researchers alike, offering a user-friendly platform for engaging with astroparticle physics. There are plenty of experiments available with this type of instrument and we showed only a few in this paper. Beyond their initial construction, GMTs-based detectors offer versatility in their applications. With the development of software applications like AstroRad for data logging and analysis, or other solutions involving microcontrollers, these detectors can serve as powerful tools for scientific research. Students can gain hands-on experience in physics, electronics, and data analysis through the construction and operation of muon detectors. These educational opportunities cultivate curiosity and critical thinking skills, laying the foundation for future scientific pursuits.

Supplementary Materials: The following supporting information can be downloaded at: https://www.mdpi.com/article/10.3390/particles7030034/s1.

Author Contributions: Conceptualization, M.A.; methodology, M.A.; software, M.A.; validation, M.A., D.L. and O.D.M.; formal analysis, M.A., D.L. and A.F.; investigation, M.A., D.L. and A.F.; resources, M.A.; data curation, M.A., D.L. and A.F.; writing—original draft preparation, M.A.; writing—review and editing, M.A., D.L., A.R.M.N., O.D.M. and C.G.; visualization, M.A., D.L., A.R.M.N., O.D.M. and C.G.; supervision, C.G. All authors have read and agreed to the published version of the manuscript.

Funding: This research received no external funding.

Data Availability Statement: The raw data supporting the conclusions of this article will be made available by the authors on request.

Acknowledgments: We acknowledge the support given by MOCRIS—a project carried out by Liceo Scientifico di Cariati (CS) in collaboration with ABProject Space; the OCRA-INFN collaboration; The high-energy group of the Department of Physics at UNICAL University; the ADA Project; and Arpacal in Catanzaro. We also acknowledge Gruppo Astronomico Tradatese (GAT), 21049 Tradate; Unione Biellese Astrofili (UBA), 13897 Occhieppo Inferiore; and Gen. Elia Rubino, Associazione Arma Aeronautica (AAA), 81100 Sezione di Caserta. Further, we acknowledge the NMDB database (www.nmdb.eu), founded under the European Union's FP7 programme (contract no. 213007) for providing data, and the PIs of individual neutron monitors at IGY Jungfraujoch (Physikalisches Institut, University of Bern, Switzerland).

Conflicts of Interest: The authors declare no conflicts of interest.

Appendix A

Solar cycles are periodic changes in the activity of the Sun. These cycles are driven by the strength of the Sun's magnetic field, usually last about 11 years, and are characterized by fluctuations in sunspot numbers, solar eruptions, and solar radiation. Solar eruptions like coronal mass ejection (CME) or solar flares can significantly impact space weather and can affect Earth's technology and climate. Solar activity influences the intensity of cosmic rays reaching Earth; during solar maximum, increased solar wind and magnetic field strength deflect more cosmic rays, reducing their intensity. Currently, we are in Solar Cycle 25, which began in December 2019. Monitoring cosmic rays is a good indicator for understanding and predicting solar activity and its effects on our planet. The current activity of the solar cycle shows a kind of plateau, as can be seen from the sunspot number index plotted by NOAA (Figure A1).

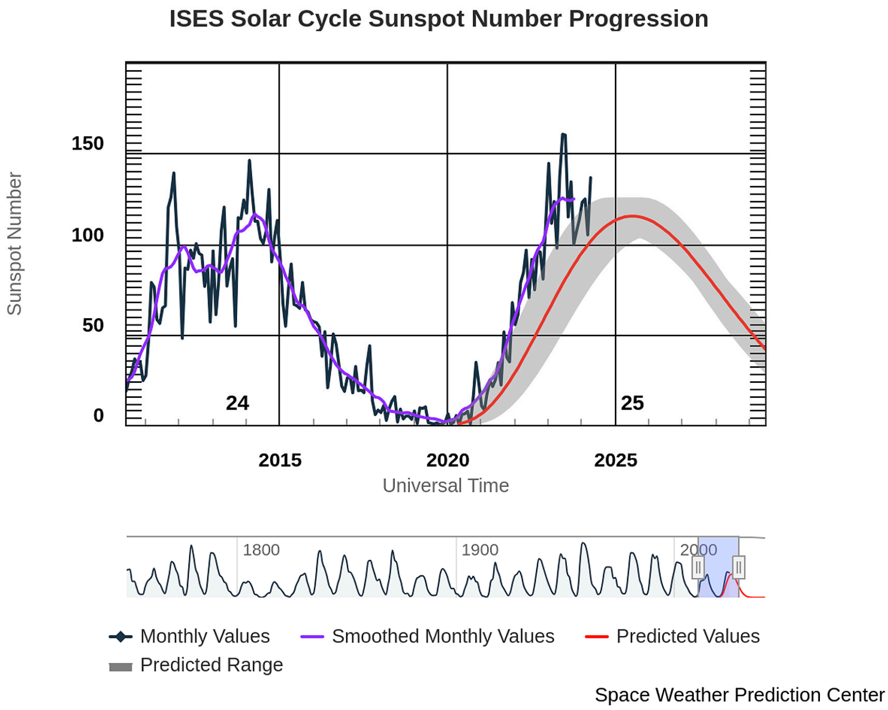

Figure A1. Progression of solar cycles 24 and 25 as sunspot number (retrieved from SWPC_NOAA on 18 May 2024).

Our best detector shows a slight increase in the muon data over the last few months (Figure A2). This could suggest a drop or a steady state of the Sun.

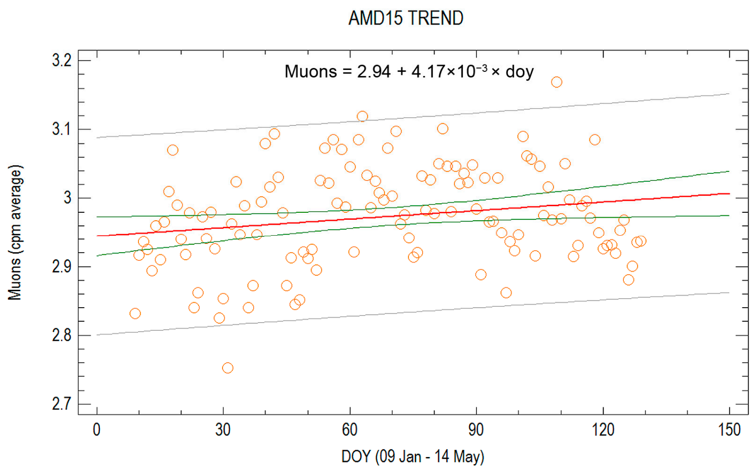

Figure A2. Daily trend of muons recorded by the AMD15 detector from January to May 2024. Orange dots represent the daily average, and the red line represents the linear regression.

Other data from the NMDB network (cosmic neutron monitors) show different trends (Figure A3). The typical shape of a solar cycle often reveals a two-peak pattern (e.g., see cycle 24), so there is a good chance that we are at the top of the first peak of the current cycle 25. Actually, the sun is currently very active; a recent solar flare produced auroras visible at low latitudes in many parts of the world.

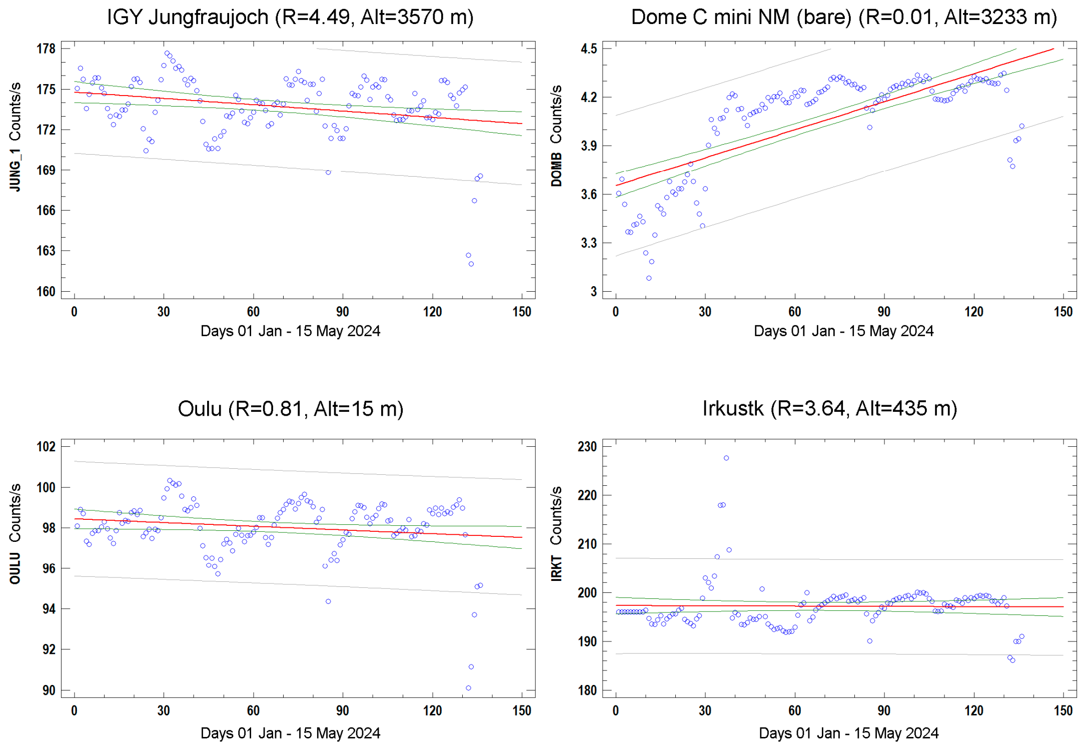

Figure A3. Plots of cosmic neutron counts from some detectors of the NMDB network (IGY Jungfraujoch, Switzerland; Dome C, Antarctica; Oulu, Finland; Irkutsk, Russia). Blue dots represent the daily averages, and the red lines represent the linear regressions; "R" indicates the value for the local magnetic rigidity.

References

1. PDG. Available online: https://pdg.lbl.gov/2005/reviews/passagerpp.pdf (accessed on 5 July 2024).
2. Bonolis, L. Walther Bothe and Bruno Rossi: The birth and development of coincidence methods in cosmic-ray physics. *Am. J. Phys.* **2011**, *79*, 1133–1150. [CrossRef]
3. Korff, S.A. *Electron and Nuclear Counters Theory and Use*; D. Van Nostrand Company, Inc.: Berlin, Germany, 1946; pp. 68–70.
4. Axani, S.N.; Frankiewicz, K.; Conrad, J.M.J. The CosmicWatch Desktop Muon Detector: A self-contained, pocket sized particle detector. *J. Instrum.* **2018**, *13*, P03019. [CrossRef]
5. Available online: http://cosmicpi.org/ (accessed on 7 June 2024).
6. Huang, N.C. Low Cost Muon Telescope (LOCOMOTE). In Proceedings of the 38th International Cosmic Ray Conference (ICRC2023), Nagoya, Japan, 26 July–3 August 2023; p. 1619. [CrossRef]
7. Bocci, V.; Chiodi, G.; Iacoangeli, F.; Nuccetelli, M.; Recchia, L. The ArduSiPM a compact trasportable Software/Hardware Data Acquisition system for SiPM detector. In Proceedings of the 2014 IEEE Nuclear Science Symposium and Medical Imaging Conference (NSS/MIC), Seattle, WA, USA, 8–15 November 2014; pp. 1–5. [CrossRef]
8. Maghrabi, A.; Makhmutov, V.S.; Almutairi, M.; Aldosari, A.; Altilasi, M.; Philippov, M.V.; Kalinin, E.V. Cosmic ray observations by CARPET detector installed in central Saudi Arabia-preliminary results. *J. Atmos. Sol. Terr. Phys.* **2020**, *200*, 105194. [CrossRef]
9. Su, S.-C.; Chen, Y.-C.; Nam, J.; Chen, P.; Kuo, C.-Y. Development of Affordable and Compact Muon Tomography Detector. In Proceedings of the 38th International Cosmic Ray Conference (ICRC2023), Nagoya, Japan, 26 July–3 August 2023; p. 531. [CrossRef]
10. Arcani, M.; Guaita, C.; Paganoni, A. VHANESSA expedition. *Astropart. Phys.* **2014**, *53*, 100–106. [CrossRef]
11. Arcani, M.; Conte, E.; Monte, O.D.; Frassati, A.; Grana, A.; Guaita, C.; Liguori, D.; Nemolato, A.R.M.; Pigato, D.; Rubino, E. The Astroparticle Detectors Array—An Educational Project in Cosmic Ray Physics. *Symmetry* **2023**, *15*, 294. [CrossRef]
12. Rossi, B. *Cosmic Rays*; McGraw-Hill: New York, NY, USA, 1964; pp. 68–73.
13. Rajpoot, H.C. HCR's Theory of Polygon (proposed by Harish Chandra Rajpoot) solid angle subtended by any polygonal plane at any point in the space. *Int. J. Math. Phys. Sci. Res.* **2014**, *2*, 28–56.
14. Janossy, L. *Cosmic Rays*; Oxford University Press: London, UK, 1948; pp. 48–49.
15. Grieder, P.K.F. (Ed.) Cosmic Ray Properties, Relations and Definitions. In *Cosmic Rays at Earth*; Elsevier: Amsterdam, The Netherlands, 2001; Chapter 1, p. 25, ISBN 9780444507105.
16. Grieder, P.K.F. (Ed.) Cosmic Rays In The Atmosphere. In *Cosmic Rays at Earth*; Elsevier: Amsterdam, The Netherlands, 2001; Chapter 2, p. 102, ISBN 9780444507105.

17. Grieder, P.K.F. (Ed.) Cosmic Rays At Sea Level. In *Cosmic Rays at Earth*; Elsevier: Amsterdam, The Netherlands, 2001; Chapter 3, p. 432, ISBN 9780444507105.
18. Radiation Detector DIY Kit. Available online: http://f4fdw.free.fr/geiger/DIY%20Geiger%20Counter%20Radiation%20Detector%20Kit%20ver.2.pdf (accessed on 10 May 2024).
19. Geiger-Counter-Radiation D-v1.1-CAJOE. Available online: https://github.com/SensorsIot/Geiger-Counter-RadiationD-v1.1-CAJOE-/tree/master (accessed on 10 May 2024).
20. Hütten, M.; Karg, T.; Schwerdt, C.; Steppa, C.; Walter, M. The International Cosmic Day—An Outreach Event for Astroparticle Physics. In Proceedings of the 35th International Cosmic Ray Conference (ICRC2017), Busan, Republic of Korea, 10–20 July 2017; p. 405. [CrossRef]
21. Acero, M.A.; Adamson, P.; Aliaga, L.; Anfimov, N.; Antoshkin, A.; Arrieta-Diaz, E.; Asquith, L.; Aurisano, A.; Back, A.; Backhouse, C.; et al. Seasonal variation of multiple-muon cosmic ray air showers observed in the NOvA detector on the surface. *Phys. Rev. D* **2021**, *104*, 012014. [CrossRef]
22. Arcani, M.; Liguori, D.; Grana, A. Exploring the Interaction of Cosmic Rays with Water by Using an Old-Style Detector and Rossi's Method. *Particles* **2023**, *6*, 801–818. [CrossRef]
23. Liguori, D. MoCRiS: A stratospheric project for an innovative approach to science education. *Teach. Methods Sci.* **2023**, *1*, 7–12. [CrossRef]
24. Hess, F. Uber Beobachtungen der durchdringenden Strahlung bei sieben Freiballonfahrten. *Phys. Z.* **1912**, *13*, 1084–1091.
25. Regener, E.; Pfotzer, G. Intensity of the Cosmic Ultra-Radiation in the Stratosphere with the Tube-Counter. *Nature* **1934**, *134*, 325. [CrossRef]
26. Regener, E.; Pfotzer, G. Vertical Intensity of Cosmic Rays by Threefold Coincidences in the Stratosphere. *Nature* **1935**, *136*, 718–719. [CrossRef]
27. Holovatyy, A.; Teslyuk, V.; Kryvinska, N.; Kazarian, A. Development of Microcontroller-Based System for Background Radiation Monitoring. *Sensors* **2020**, *20*, 7322. [CrossRef] [PubMed]
28. United Nations Scientific Committee on the Effects of Atomic Radiation. *Sources and Effects of Ionizing Radiation–Volume 1*; United Nations: New York, NY, USA, 2010; p. 4, ISBN 978-92-1-142274-0. Available online: https://www.unscear.org/unscear/uploads/documents/unscear-reports/UNSCEAR_2008_Report_Vol.I-CORR.pdf (accessed on 16 May 2024).
29. Restier-Verlet, J.; El-Nachef, L.; Ferlazzo, M.L.; Al-Choboq, J.; Granzotto, A.; Bouchet, A.; Foray, N. Radiation on Earth or in Space: What Does It Change? *Int. J. Mol. Sci.* **2021**, *22*, 3739. [CrossRef] [PubMed]